NONLINEAR FE MODEL UPDATING FOR MASONRY CONSTRUCTIONS VIA LINEAR PERTURBATION AND MODAL ANALYSIS

Maria Girardi[1]**, Cristina Padovani**[1]**, Daniele Pellegrini**[1]**, and Leonardo Robol**[2,1]

[1]Institute of Information Science and Technologies "A. Faedo" (ISTI-CNR)
Via G. Moruzzi 1, Pisa, Italy
e-mail: {maria.girardi, cristina.padovani, daniele.pellegrini}@isti.cnr.it

[2] Department of Mathematics, University of Pisa
Largo Bruno Pontecorvo 5, Pisa, Italy
e-mail: leonardo.robol@unipi.it

Keywords: Masonry materials, Nonlinear elasticity, Linear perturbation, Modal analysis, Nonlinear Model updating.

Abstract.   *This paper describes the automated nonlinear model updating procedure for masonry structures implemented in the NOSA-ITACA code. The algorithm, aimed at matching numerical and experimental natural frequencies and mode shapes, combines nonlinear static analysis, linear perturbation and modal analysis and allows fine-tuning the free parameters of the model. The numerical method is applied to two simple case studies, which prove its effectiveness.*

1 INTRODUCTION

The goals of finite element (FE) model updating [1] are matching numerical and experimental dynamic characteristics of a structure, estimating the mechanical properties of its constituent materials [2, 3, 4, 5], and enabling detection of damage [6, 7]. Model updating, usually carried out within the framework of linear elasticity, is a suitable tool for assessing the mechanical characteristics of undamaged structures subjected to very low amplitude vibrations, while it is unsuitable to update parameters governing nonlinear behavior and/or material properties deterioration. Therefore, the use of model updating techniques within the framework of linear elasticity may be not suitable for masonry structures, since the masonry material has different tensile and compressive strengths and then exhibit a nonlinear behavior. Generally ancient masonry structures show cracks due to permanent loads and / or accidental loads, therefore, the characterization of their overall dynamic behavior should take into account the presence of the existing fracture pattern.

To date, the literature on nonlinear FE model updating is quite scarce. The first attempts to update in a systematic way nonlinear models mainly concerns reinforced concrete structures. In [8] a system identification methodology is presented for determining the six control parameters in a continuously smooth hysteretic model for the inelastic dynamic behavior of structural concrete systems, while in [9] the authors use low-level ambient vibration data to detect changes in the modal parameters of a reinforced concrete shear wall. Then, the damage parameters that control the nonlinear material model are updated using the acquired modal information. Finally, in [10] the performance of a nonlinear model updating procedure is investigated in the case of a concrete seven-story shear wall building.

With regard to masonry structures, in [11, 12, 13] the dynamic behavior of masonry buildings is assessed using a numerical procedure based on linear perturbation and modal analysis, implemented in the FE code NOSA-ITACA, taking into account the influence of existing damage on the dynamic properties of buildings. In [14, 15] the same approach is followed to estimate Young's moduli and tensile strengths of the materials constituting the Mogadouro bell tower, by applying a manual nonlinear model updating procedure.

This paper presents a novel automated nonlinear model updating procedure, implemented in the NOSA-ITACA code. The algorithm, aimed at matching numerical and experimental frequencies and mode shapes, couples linear perturbation and modal analysis and allows fine-tuning the free parameters of the model. After a brief description of the numerical method proposed, its effectiveness is demonstrated on some simple case studies.

2 NUMERICAL METHODS FOR NONLINEAR MODEL UPDATING

The NOSA-ITACA code adopts the constitutive equation of masonry-like materials [16, 17] and masonry is modeled as an isotropic nonlinear elastic material with low tensile strength and infinite compressive strength. The material nonlinearity brings as consequence a stronger nonlinearity of the model updating procedure implemented in NOSA-ITACA. This procedure relies on the combined application of linear perturbation and modal analysis, which allows to calculate the dynamic properties of a structure, taking the presence of cracks into account. Given the structure under examination, discretized into finite elements, and given the mechanical properties of the masonry-like material constituting the structure, together with the kinematic constraints and loads acting on it, the coupled application of linear perturbation and modal analysis consists of the following steps.

Step 1. The nonlinear equilibrium problem of the structure is solved through an iterative

scheme and its solution is calculated along with the tangent stiffness matrix $\mathbf{K_T}$ to be used in the next step.

Step 2. A modal analysis about the equilibrium solution is performed. The dynamic properties of the structures are then calculated by solving the generalized eigenvalue problem

$$\mathbf{K_T}\,\mathbf{v} = \omega^2\,\mathbf{M}\,\mathbf{v}; \tag{1}$$

where $\mathbf{v} \in \mathbb{R}^n$ is the vector of the structure's degrees of freedom and the integer n is the system's total number of degrees of freedom. Matrices $\mathbf{K_T} \in \mathbb{R}^{n \times n}$ and $\mathbf{M} \in \mathbb{R}^{n \times n}$ are the stiffness and mass matrices, symmetric and positive-definite, obtained by assembling the elemental matrices and taking into account the constraints assigned to the displacements of the structure. Solving (1) provides the natural frequencies $f_i = \omega_i/2\pi$ and mode shapes $\mathbf{v}^{(i)}$ of the cracked structure [11, 12, 13]. The nonlinear model updating problem can be formulated as an optimization problem by assuming that the tangent stiffness and mass matrices are functions of the parameter vector $\mathbf{x}$, containing the Young's moduli, tensile strengths and density masses of the constituent materials. The goal is to determine the optimal value of $\mathbf{x} \in \mathbb{R}^d$ that minimizes a certain cost functional $\Phi(\mathbf{x})$ within a d-dimensional box $\Omega = [a_1, b_1] \times \ldots \times [a_d, b_d]$. The objective function $\Phi(\mathbf{x})$ involves the q experimental frequencies to match and is expressed by

$$\Phi(\mathbf{x}) = \sum_{i=1}^{q} w_i^2 [\widehat{f_i} - f_i(\mathbf{x})]^2, \tag{2}$$

with $\widehat{\mathbf{f}}$ the vector of the measured frequencies, $\mathbf{f}(\mathbf{x})$ the vector of numerical frequencies obtained from (1) and w_i suitable weights.

A numerical method for FE model updating of structures made of linear elastic materials has been described in [18, 19]. The minimum problem addressed in [18, 19] is a nonlinear least squares problem: the objective function, having the form (2), is nonlinear as the frequencies $\mathbf{f}(\mathbf{x})$ depend nonlinearly on the vector $\mathbf{x}$ of material properties. In this paper, another source of nonlinearity of $\Phi(\mathbf{x})$ is the dependence of $\mathbf{K_T}(\mathbf{x})$, and then of $\mathbf{f}(\mathbf{x})$, on the solution of the equilibrium problem in step (1).

This section is devoted to the description of the method adopted to optimize the objective function $\Phi(\mathbf{x})$, which is assumed to have at least a mild regularity in Ω. Apart from the determination of the initial box constraints, any convexity or uniqueness of the minimum point cannot be assumed. For this reason, a method that guarantees good global convergence properties is used.

In particular, a method based on an adaptive global polynomial interpolation of the objective function is proposed, which helps to avoid the convergence to local minima. The main building block of this approach is the approximation of multivariate functions through Chebsyhev interpolation combined with adaptive cross approximation techniques, as implemented in the packages `chebfun2` and `chebfun3` [20, 21].

The algorithms implemented in NOSA-ITACA are based on those described in [20, 21], and allow to manage a generic number of variables, as well as to get approximations at different levels of precisions. The details of the implementation are given in [22]. In the next sections the building blocks of our method are briefly explained, and then the approach is summarized in section 2.3.

2.1 Global approximation of the objective function

As a building block of the optimization method, we use a procedure that allows to approximate the objective function on the whole domain at a certain accuracy ϵ. More precisely, we ask that the surrogate function $\Phi_k(\mathbf{x})$ satisfies

$$\Phi(\mathbf{x}) = \Phi_k(\mathbf{x}) + r_k(\mathbf{x}), \qquad |r_k(\mathbf{x})| \leq \max_{\mathbf{z} \in \Omega} |\Phi(\mathbf{z})| \epsilon. \tag{3}$$

To obtain such $\Phi_k(\mathbf{x})$ we approximate the function as the sum of k separable functions as follows:

$$\Phi(\mathbf{x}) \approx \Phi_k(\mathbf{x}) = \sum_{j=1}^{k} \beta_j \varphi_1^{(j)}(x_1) \cdots \varphi_d^{(j)}(x_d), \tag{4}$$

where the functions $\varphi_i^{(j)}(x_i)$ are expressed as polynomials in the Chebyshev basis. This can be achieved as follows:

1. A pivot point $\hat{\mathbf{x}} := (\hat{x}_1, \ldots, \hat{x}_d)$ is chosen, and the function $\Phi(\hat{x}_1, \ldots, \hat{x}_d)$ is evaluated at that point.

2. Through adaptive Chebyshev interpolation, we approximate the fibers of $\Phi(\mathbf{x})$ obtained allowing only one variable to change, that is

$$\Phi(\hat{x}_1, \ldots, \hat{x}_{i-1}, y, \hat{x}_{i+1}, \ldots, \hat{x}_d) \approx \sum_{s=1}^{k_i} \gamma_s T_s(y) =: \varphi_i^{(1)}(y), \qquad i = 1, \ldots, d. \tag{5}$$

   where $T_s(y)$ are the Chebyshev polynomials of the first kind, and k_i is a positive integer that is adaptively determined to obtain a sufficiently accurate expansion. The coefficients γ_s can be efficiently computed through a discrete cosine transform [20].

3. We set $\beta_1 := \Phi(\hat{\mathbf{x}})^{1-d}$.

Clearly, the function $\beta_1 \varphi_1^{(1)}(x_1) \cdots \varphi_d^{(d)}(x_d)$ corresponds with $\Phi(\mathbf{x})$ on $\hat{\mathbf{x}}$. This first separable approximation is known as a rank-1 function. After the first step is complete, we replace $\Phi(\mathbf{x})$ with the residual $\Phi(\mathbf{x}) - \beta_1 \varphi_1^{(1)}(x_1) \cdots \varphi_d^{(d)}(x_d)$ and we repeat the steps from item 1. After k steps, we have obtained an expression of the form (4).

This approach is called *functional adaptive cross approximation*, and has been investigated, among others, by Bebendorf [23] and in [24, 25, 26] for bivariate functions. It can be guaranteed to converge under suitable assumptions on the smoothness of the functions under consideration, provided that good choices are made for the pivots.

Greater details on how to build such an approximation of Φ and on the effectiveness of the approach are given in [22].

2.2 Computing the minimum

When the approximated function is available in the form $\Phi_k(\mathbf{x})$, its global minimum has to be calculated. To this end, several possibilities can be considered, exploiting the fact that $\Phi_k(\mathbf{x})$ is much cheaper to evaluate compared to $\Phi(\mathbf{x})$. In our implementation, we make the following choices:

1. If $d = 2$, we compute all the stationary points of the polynomial in the domain of interest, by solving the system of 2 polynomial equations $\nabla\Phi_k(\mathbf{x}) = 0$. The nature of the problem imposes a numerical solution, which can be obtained recasting the problem as a *multi-parameter eigenvalue problem* [27]; we then use this information to select the minimum point.

2. If $d \geq 3$, we use the fact that the approximated function is cheap to evaluate and we evaluate it on a grid, and then refine the minimum found in this way by using a local optimization method.

In principle, the first approach could be used also when $d > 2$ (see recent linearizations introduced in [28, 29]). However, as the number of variables gets higher, the reformulation into an eigenvalue problem can get exponentially ill-conditioned [30]. We expect that for a large number of variable a strategy like 2. would be more effective and has been adopted for $d = 3$ as well.

2.3   Algorithm propose: combining global and local approximation

The algorithm we propose can be summarized as follows:

1. First, we obtain a very rough approximation of the objective function $\Phi(\mathbf{x})$ on Ω (for instance, we may set $\epsilon = 0.1$ in (3)) and denote this approximation with $\Phi_k(\mathbf{x})$.

2. Then, we look for the minimum point $\hat{\mathbf{x}}$ of this approximated function and we compute intervals $[\hat{a}_j, \hat{b}_j]$ as large as possible, with the constraints that $a_j \leq \hat{a}_j < \hat{b}_j \leq b_j$, and

$$\Phi_k(\hat{x}_1, \ldots, \hat{x}_{j-1}, y, \hat{x}_{j+1}, \ldots, \hat{x}_d) - \Phi_k(\hat{\mathbf{x}}) \leq \max_{\mathbf{z} \in \Omega} |\Phi_k(\mathbf{z})| \cdot \hat{\epsilon}, \tag{6}$$

for any $y \in [\hat{a}_j, \hat{b}_j]$, and for a certain $\hat{\epsilon}$.

3. We restrict Ω to $\hat{\Omega} = [\hat{a}_1, \hat{b}_1] \times \ldots \times [\hat{a}_d, \hat{b}_d]$, and we continue to iterate from point 1.

This process allows to obtain a rough approximation of the global minimum, and then restricts the interval of interest to points where the objective function does not exceed too much its value at $\hat{\mathbf{x}}$. The restriction is done by computing a new box as described above in point 2. Note that, from a theoretical point of view, this strategy does not guarantee that the global minimum will be inside the new box. However, if $\hat{\epsilon}$ is chosen slightly larger than ϵ, the global convergence properties of the method are still very good in practice.

In the tests described in section 3 we have used $\hat{\epsilon} = 2\epsilon$, which has been verified to be a reasonable tradeoff between speed of convergence and accuracy (in the sense of not leaving global minimum out of the restricted $\hat{\Omega}$).

3   CASE STUDIES

In order to validate the performance of the optimization method described in section 2, two artificial examples are used. In both cases a preliminary numerical analysis consisting of static analysis, linear perturbation and modal analysis (from now on indicated as LPMA), is performed to evaluate the frequencies and mode shapes of the structure, taking into account the crack pattern due to the self-weight and external loads [11, 12, 14]. Subsequently, these frequencies are used as input of the proposed approach to recover the original parameters (Young's moduli and/or tensile strengths).

3.1 Masonry arch

Let us consider the semi-circular masonry arch sketched up in Figure 1. The system is fully clamped at the springings and its geometry is characterized by a mean radius of 1.0 m, a span of 2.0 m and a cross section of 0.25 m $\times 1$ m. The displacement of the arch along the X direction is prevented so that it is forced to move only in the YZ plane. The arch is subjected to a stress state due to its self-weight and to a distributed load P $= 2500$ N/m applied along the extrados line Y $= 0.29$ m, Z $= 1.09$ m. The arch is discretized into 648 thick shell elements (element number 10 of the NOSA-ITACA library [31]), for a total of 703 nodes and 4218 degrees of freedom. Figure 1 shows the mesh generated by NOSA-ITACA, and the distributed load applied to the arch. A preliminary LPMA is performed to evaluate the frequencies and mode shapes of the arch, taking into account the crack pattern due to the self-weight and distributed load P; the analysis is performed assuming the arch made of a masonry-like material [16, 17] with Young's modulus $E = 3 \cdot 10^9$ Pa, Poisson's ratio $\nu = 0.1$, mass density $\rho = 1800$ kg/m^3 and tensile strength $\sigma_t = 0$ Pa. The first four corresponding natural frequencies $\widehat{f}_i$ (i $= 1...4$), obtained with the above parameters are

$$\widehat{\mathbf{f}} = [42.913, 97.321, 138.630, 184.199] \text{ Hz}. \tag{7}$$

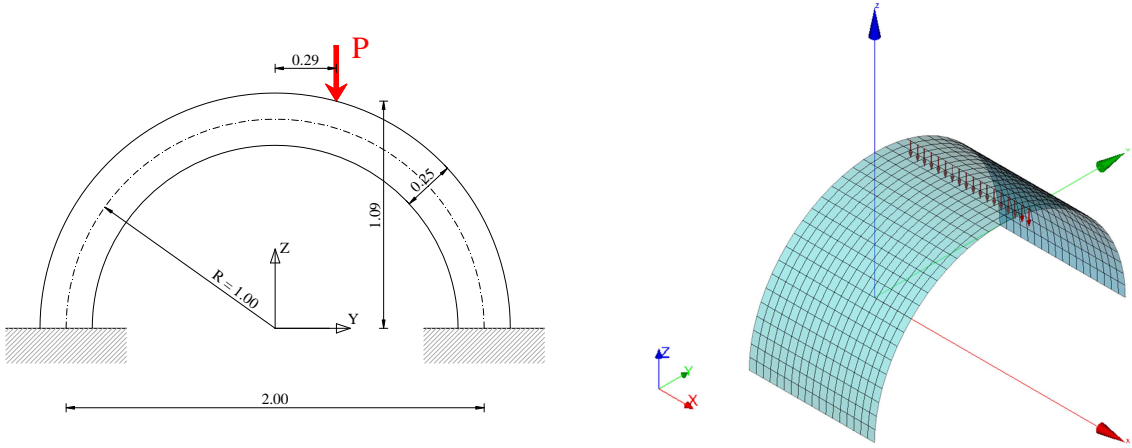Figure 2 shows the mode shapes corresponding to the first four frequencies of the arch.

Figure 1: Geometry of the arch (length in meters) and mesh created by NOSA-ITACA.
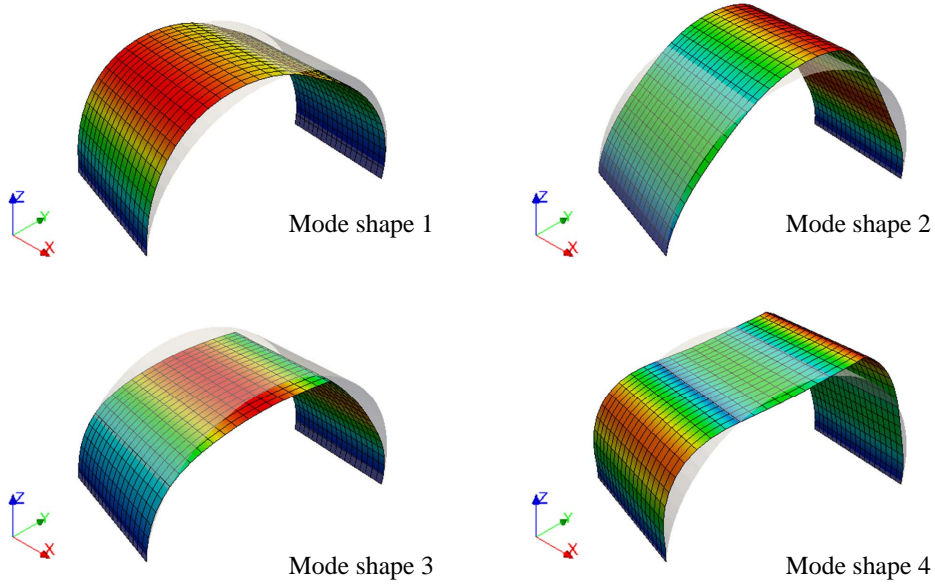
Figure 2: First four mode shapes of the arch after the application of the self-weight and distributed load P.

In order to validate the optimization method we minimize the objective function (2), with $q = 3$, $\widehat{f}_1 = 42.913$ Hz, $\widehat{f}_2 = 97.321$ Hz, and $\widehat{f}_3 = 138.630$ Hz, and $w_\mathrm{i} = \widehat{f}_\mathrm{i}^{-1}$, $\mathrm{i} = 1, 2, 3$. The tensile strength σ_t and the Young's modulus E are assumed unknown, considering as their realistic bounds the following ranges

$$0 \text{ Pa} \leq \sigma_t \leq 5 \cdot 10^4 \text{ Pa}, 1 \cdot 10^9 \text{ Pa} \leq E \leq 5 \cdot 10^9 \text{ Pa} \cdot \tag{8}$$

The algorithm described in section 2.3 converges in 3 iterations to the prescribed tolerance $\epsilon = 2 \cdot 10^{-2}$. The optimal parameters obtained are reported in Table 1. The estimate for E is very accurate with a relative error of about 0.1%, while the value of σ_t is very close to zero in practice. The error Δ_f on the frequencies is bounded by about 0.38% and MAC values equal to 1.0 ensures the correspondence between original and optimized mode shapes (see Table 2). Figure 3 shows the objective function $\Phi(\mathbf{x})$ where several local minima are also visible, while the true global minimum corresponds to a point where there is a steep descent. For this reason, classical algorithms for nonlinear least square problems fail to find the right value of σ_t – whereas the approach proposed in section 2 yields a good solution.

	E [Pa]	σ_t [Pa]
true	$3.0 \cdot 10^9$	0.0
optimal	$3.003 \cdot 10^9$	80.4
error [%]	0.1%	–

Table 1: Comparison between the true values of the mechanical characteristics and those obtained from optimization.

7

	$\widehat{f}_i$ [Hz]	$f_{i,O}$ [Hz]	$\Delta_f[\%]$	MAC
mode 1	42.913	43.077	0.38%	1.0
mode 2	97.321	97.387	0.07%	1.0
mode 3	138.630	138.915	0.21%	1.0
mode 4	184.199	184.189	0.06%	1.0

Table 2: Comparison between the original frequencies $\widehat{f}_i$ and the frequencies $f_{i,O}$ calculated for the optimal values of the parameters.
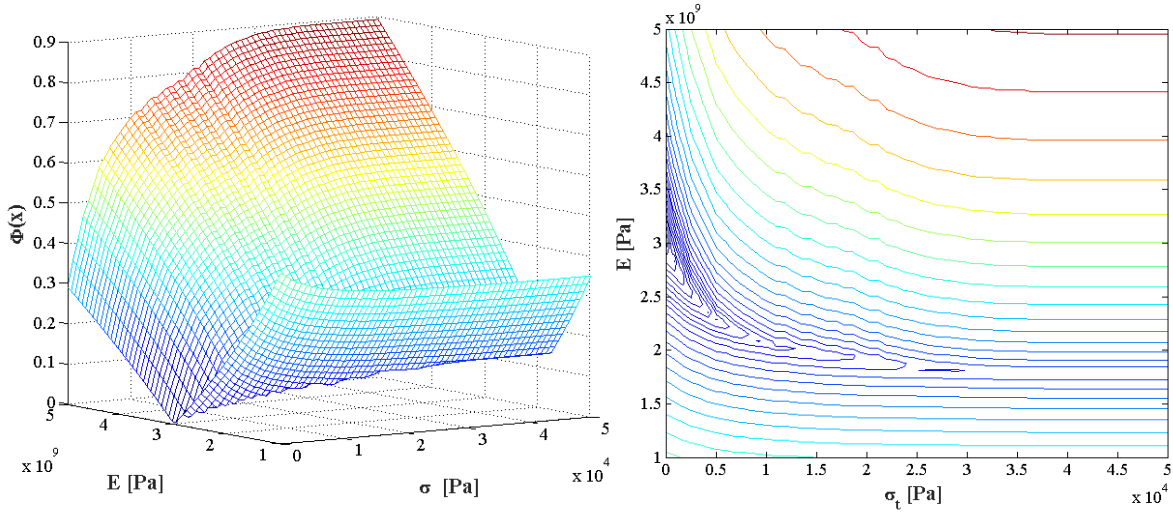

Figure 3: On the left, a 3D plot of the objective function for the case study of the arch. On the right, a contour plot of the same objective function, where local minima and flat regions are clearly visible.

3.2   Masonry arch on piers

The second example considered is the semi-circular arch on piers shown in Figure 4. The arch spans 2.0 m, has a cross section of 0.25 m $\times$ 1 m and rests on two 2.5 m high lateral piers having cross section of 0.5 m $\times$ 1 m. The structure is fully clamped at the base of the piers and subjected to a stress state due to its self-weight and to a lateral load proportional to its mass through a factor equal to 0.15g, where g is the gravity acceleration. The structure is discretized into 1008 thick shell elements (element number 10, [31]), for a total of 1083 nodes and 6498 degrees of freedom, as shown in Figure 4.
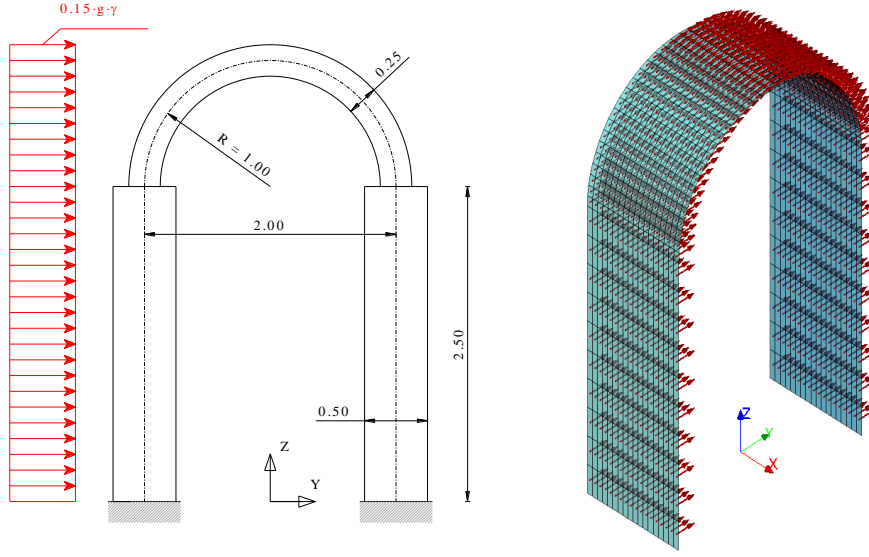
Figure 4: Geometry of the structure (length in meters) and the model created by NOSA-ITACA.

A LPMA is performed assuming the structure made of two masonry-like materials with the same Young's modulus and different tensile strengths: the material 1 of the arch and the material 2 of the columns. The Poisson's ratio is set to $\nu = 0.2$ for all the materials, and assumed to be known a priori. For the remaining parameters the following values are assumed

$$E = 2.0 \cdot 10^9 \text{ Pa}, \rho_1 = 1800 \text{ kg/m}^3, \sigma_{t,1} = 1 \cdot 10^4 \text{ Pa} \tag{9}$$

$$E = 2.0 \cdot 10^9 \text{ Pa}, \rho_2 = 2200 \text{ kg/m}^3, \sigma_{t,2} = 4 \cdot 10^4 \text{ Pa} \tag{10}$$

The first six natural frequencies $\widehat{f}_i$ (i = 1...6), obtained with these fixed parameters are:

$$\widehat{\mathbf{f}} = [3.124,\ 9.083,\ 10.46,\ 14.83,\ 15.60,\ 24.57] \text{ Hz} \cdot \tag{11}$$

Figure 5 shows the mode shapes corresponding to the first four frequencies of the structure.
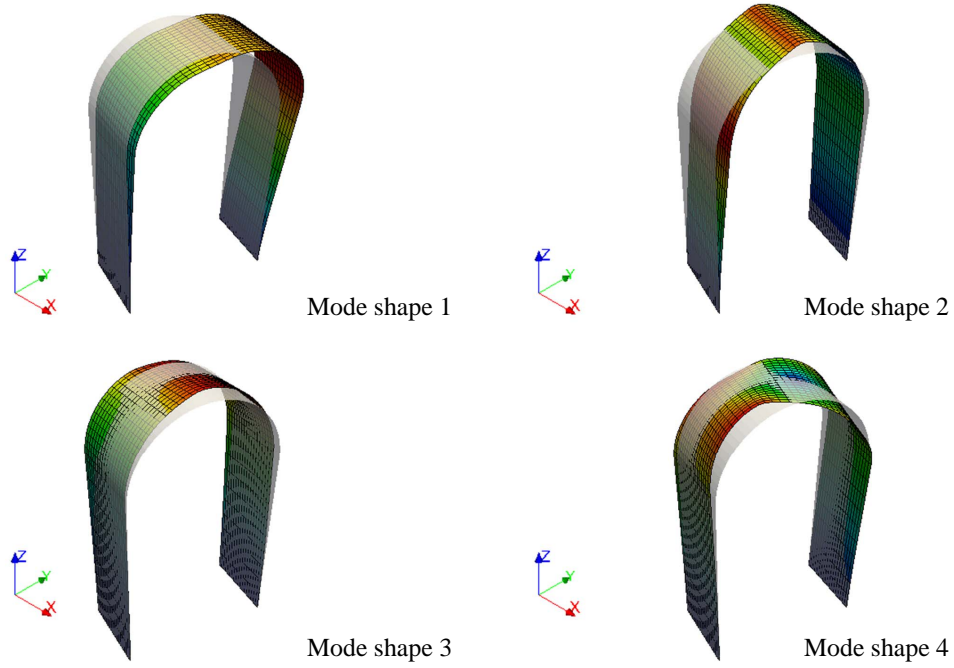
Figure 5: First four mode shapes of the system arch-piers after the application of the self-weight and lateral load.

In order to validate the optimization method, the tensile strength $\sigma_{t,1}$ and $\sigma_{t,2}$ and Young's modulus E are assumed unknown considering, as their realistic bounds the following ranges

$$1 \cdot 10^4 \text{ Pa} \leq \sigma_{t,1}, \sigma_{t,2} \leq 5 \cdot 10^4 \text{ Pa}, 1 \cdot 10^9 \text{ Pa} \leq E \leq 5 \cdot 10^9 \text{ Pa} \cdot$$

The method applied to the objective function (2) with $q = 6$ converges in 7 iterations to the optimal values reported in Table 3 with a maximum relative error of 2.31% and of 0.7% for the Young's modulus and tensile strength respectively. Table 4 shows the results in terms of natural frequencies and MAC values with a maximum relative error Δ_f of 1% on frequencies and a minimum value of MAC equal to 0.99.

	E [Pa]	$\sigma_{t,1}$ [Pa]	$\sigma_{t,2}$ [Pa]
true	$2 \cdot 10^9$	10^4	$4 \cdot 10^4$
optimal	$1.9538 \cdot 10^9$	10^4	$4.028 \cdot 10^4$
error [%]	2.31%	0%	0.7%

Table 3: Comparison between the true values of the mechanical characteristics and those obtained from optimization.

	$\widehat{f}_\mathrm{i}$ [Hz]	$f_\mathrm{i,O}$ [Hz]	$\Delta_f[\%]$	MAC
mode 1	3.124	3.122	0.04	1.000
mode 2	9.083	9.004	0.87	0.999
mode 3	10.459	10.379	0.76	1.000
mode 4	14.834	14.795	0.26	0.999
mode 5	15.595	15.441	0.99	1.000
mode 6	24.566	24.411	0.63	0.999

Table 4: Comparison between the original frequencies $\widehat{f}_\mathrm{i}$ and the frequencies $f_\mathrm{i,O}$ calculated for the optimal values of the parameters.

4 CONCLUSIONS

This paper is focussed on FE model updating of masonry structures. Unlike linear elastic structures, whose dynamic properties depend on the materials' characteristics, such as Young's modulus, mass density, etc., masonry buildings exhibit a nonlinear behavior and their natural frequencies and mode shapes are not independent of crack distribution. The numerical procedure presented in the paper takes into account the nonlinearity of masonry materials. After solving the nonlinear equilibrium problem of the structure subjected to prescribed loads, a modal analysis about the equilibrium solution is carried out to estimate its frequencies and mode shapes in the presence of cracks. The model updating algorithm allows for minimizing the discrepancy between the experimental and numerical frequencies, as the materials' constants vary within a given set. As in the case of linear elastic materials addressed in [18, 19] the minimum problem to be solved is a nonlinear least squares problem. In the presence of masonry materials a further nonlinearity, due to the dependence of the tangent stiffness matrix on the solution to the equilibrium problem, affects the objective function and makes it impossible to resort to the efficient model reduction techniques adopted in [18, 19]. The minimization strategy proposed in this paper is based on an adaptive global polynomial interpolation of the objective function. The approach implemented in NOSA-ITACA and applied to two simple case studies seems to be able to overcome the difficulties due to the presence of several global minima in the objective function. Further tests are planned to validate the performance of the algorithm and prove its capabilities in a broader class of numerical problems.

REFERENCES

[1] J.E. Mottershead, M.I. Friswell, Model updating in structural dynamics:a survey. *J.Sound Vib*, **167(2)**, 347–375, 1993.

[2] C. Gentile and A. Saisi, Ambient vibration testing of historic masonry towers for structural identfication and damage assessment. *Construction and Building Materials*, **21**, 1311-1321, 2007.

[3] R. M. Azzara., A. De Falco, M. Girardi, D. Pellegrini, Ambient vibration recording on the Maddalena Bridge in Borgo a Mozzano (Italy): data analysis. *Annals of Geophysics*, **60(4)**, S0441, 2017.

[4] A. Cabboi, C. Gentile, and A. Saisi, From continuous vibration monitoring to fem-based damage assessment: Application on a stone-masonry tower. *Construction and Building Materials*, **156**, 252–265, 2017.

[5] Y. S. Erdogan, Discrete and continuous finite element models and their calibration via vibration and material tests for the seismic assessment of masonry structures. *International Journal of Architectural Heritage*, **11(7)**, 1026–1045, 2017.

[6] B. Moaveni, A. Stavridis, G. Lombaert, J. Conte, P. Shing, Finite element model updating for assessment of progressive damage in a three-story infilled RC frame *J.Struct.Eng.*, **139**, 1665–1674, 2013.

[7] C. Papadimitriou, D.C. Papadioti, Component mode synthesis techniques for finite element model updating *Comput.Struct.*, **126**, 15–28, 2013.

[8] S.K. Kunnath, J.B. Mander, L. Fang, Parameter identification for degrading and pinched hysteretic structural concrete systems. *Eng.Struct*, **19(3)**, 224–232, 1997.

[9] W. Song, S. Dyke and T. Harmon Application of Nonlinear Model Updating for a Reinforced Concrete Shear Wall. *Journal of Engineering Mechanics*, **139-5**, 635–649, 2013.

[10] E. Asgarieh, B. Moaveni, A.R. Barbosa, E. Chatzi, Nonlinear model calibration of a shear wall building using time and frequency data features. *Mechanical Systems and Signal Processing*, **85**, 236–251, 2017.

[11] D. Pellegrini, M. Girardi, C. Padovani, and R. M. Azzara, A new numerical procedure for assessing the dynamic behaviour of ancient of ancient masonry towers. M. Papadrakakis, M. Fragiadakis eds. *6th International Conference on Computational Methods in Structural Dynamics and Earthquake Engineering (COMPDYN 2017)*, Rodhes Island, Greece, June 15-17, 2017.

[12] M. Girardi, C. Padovani, and D. Pellegrini, Modal analysis of masonry structures. *Mathematics and Mechanics of Solids SAGE Publications Ltd*, First published February 13, 2018.

[13] M. Girardi, C. Padovani, and D. Pellegrini, Effects of the stress field on the dynamic properties of masonry bell towers. *AIMETA 2017 - Proceedings of the XXIII Conference of the Italian Association of Theoretical and Applied Mechanics vol.1 ISBN 978-889-42484-7-0*, Salerno, Italy, September 4-7, 2017.

[14] D. Pellegrini, M. Girardi, P.B. Lourenço, M.G. Masciotta, N. Mendes, C. Padovani, L.F. Ramos, Modal analysis of historical masonry structures: linear perturbation and software benchmarking. *Construction and Building Materials*, **189**, 1232–1250, 2018.

[15] R. M. Azzara., M. Girardi, C. Padovani, D. Pellegrini, Experimental and numerical investigations on the seismic behaviour of the San Frediano bell tower in Lucca. *Annals of Geophysics*, **61**, Early paper, 2018.

[16] G. Del Piero, Constitutive equation and compatibility of external loads for linear elastic masonry–like materials *Meccanica*, **24**, 150–162, 1989.

[17] M. Lucchesi, C. Padovani, G. Pasquinelli, N. Zani, *Masonry constructions: mechanical models and numerical applications* 2008; Lecture Notes in Applied and Computational Mechanics. Springer–Verlag.

[18] M. Girardi, C. Padovani, D. Pellegrini, M. Porcelli, L. Robol, Finite element model updating for structural applications. arXiv:1801.09122 [math.NA], 2018.

[19] M. Girardi, C. Padovani, D. Pellegrini, L. Robol, A model updating procedure to enhance structural analysis in the FE code NOSA-ITACA. arXiv:1902.03949v1 [cs.CE], 2019.

[20] R. B. Platte, L. N. Trefethen, *Progress in industrial mathematics at ECMI 2008*, Springer. *Chebfun: a new kind of numerical computing*, 68–87, 2010.

[21] B. Hashemi, L. N. Trefethen, Chebfun in three dimensions. *SIAM Journal on Scientific Computing*, **39(5)**, C341–C363, 2017.

[22] M. Girardi, C. Padovani, D. Pellegrini, L. Robol, Finite element model updating for masonry structures. *in preparation*.

[23] Bebendorf, Mario, Adaptive cross approximation of multivariate functions. *Constructive approximation*, **34(2)**, 149–179, 2011.

[24] A. Townsendand, L. N. Trefethen, An extension of Chebfun to two dimensions. *SIAM Journal on Scientific Computing*, **35(6)**, C495–C518, 2013.

[25] J. Schneider. Error estimates for two-dimensional cross approximation. *Journal of approximation theory* 162.9 1685-1700, 2010

[26] A. Cortinovis, D. Kressner, S. Massei. On maximum volume submatrices and cross approximation for symmetric semidefinite and diagonally dominant matrices. arXiv:1902.02283 [math.NA], 2019.

[27] M. E. Hochstenbach, B. Plestenjak, Backward error, condition numbers, and pseudospectra for the multiparameter eigenvalue problem. *Linear algebra and its applications*, **375**, 63–81, 2003.

[28] A. Boralevi, J. van Doornmalen, J. Draisma, M. E. Hochstenbach, B. Plestenjak, Uniform determinantal representations. *SIAM journal on applied algebra and geometry*, **1(1)**, 415–441, 2017.

[29] L. Robol, R. Vandebril, P. Van Dooren, A framework for structured linearizations of matrix polynomials in various bases. *SIAM Journal on Matrix Analysis and Applications*, **38(1)**, 188–216, 2017.

[30] V. Noferini, A. Townsend, Numerical instability of resultant methods for multidimensional rootfinding. *SIAM Journal on Numerical Analysis*, **54(2)**, 719–743, 2016.

[31] V. Binante, M. Girardi, C. Padovani, G. Pasquinelli, D. Pellegrini, M. Porcelli, L. Robol, *NOSA-ITACA 1.1 documentation* 2017. www.nosaitaca.it/software/.